

Improving thermodynamic bounds using correlations

Andreas Dechant¹ and Shin-ichi Sasa¹

¹*Department of Physics #1, Graduate School of Science, Kyoto University, Kyoto 606-8502, Japan*
(Dated: September 1, 2021)

We discuss how to use correlations between different physical observables to improve recently obtained thermodynamic bounds, notably the fluctuation-response inequality (FRI) and the thermodynamic uncertainty relation (TUR). We show that increasing the number of measured observables will always produce a tighter bound. This tighter bound becomes particularly useful if one of the observables is a conserved quantity, whose expectation is invariant under a given perturbation of the system. For the case of the TUR, we show that this applies to any function of the state of the system. We demonstrate our finding on a model of the F₁-ATPase molecular motor, where we obtain a bound that is more than a factor of 2 tighter than the one given by the TUR.

I. INTRODUCTION

Entropy production is a fundamental concept of non-equilibrium statistical mechanics. It relates the asymmetry of microscopic transitions in a system to the measurable loss of energy in the form of heat dissipated into the environment. For macroscopic systems, measuring the latter thus provides a measure of microscopic time-reversal symmetry breaking. While the same relation holds for microscopic systems and can be even be formulated on the level of single trajectories [1, 2], measuring the dissipated heat is generally very challenging, as the resulting temperature changes are very small and typically lost among the fluctuations of the noisy environment. A more practical way to measure the entropy production in microscopic systems is provided by the work of Harada and Sasa [3], who show that the entropy production can be obtained from the violation of the fluctuation-dissipation relation. We remark that in principle, the entropy production may also be obtained directly from the probabilities of microscopic transitions in the system, however, this requires very good spatial and temporal resolution as well as lots of statistics.

A different way of estimating entropy production has recently been suggested [4–8] using the thermodynamic uncertainty relation (TUR) [9–12]. The TUR establishes a connection between entropy production on the one hand, and measurable currents in the system and their fluctuations on the other hand. It may be understood as a more precise formulation of the second law, since it not only establishes the positivity of entropy production but also provides a finite lower bound in terms of experimentally accessible quantities. However, since the TUR is an inequality, there is generally no guarantee that the lower bound is tight, i. e. that a useful estimate of entropy production is obtained from a given measurement. In principle the lower bound can be optimized to produce an accurate estimate of entropy production [4–7] and even realize equality [13], however, the resulting quantities may not be any easier to measure than the entropy production itself.

From an experimental point of view, it is thus highly desirable to improve the tightness of the bound using

available data. However, the tightness of the bound is also of fundamental interest: For example, it has been shown [14] that the TUR is generally not very tight for models of biological molecular motors, with the lower estimate on entropy production being on the order of 10 to 40% of the actual value. This raises the intriguing question of whether evolution is “bad” at saturating thermodynamic bounds, or whether indeed a tighter bound exists.

So far, applications and extensions of the TUR have mostly focused only on current-like observables (for example the displacement of a particle or the heat exchanged with the environment) [15–17], although it has been found [18–20] that, in the presence of time-dependent driving, also state-dependent observables (like the instantaneous position or potential energy) may yield information about the entropy production. While the presence of non-zero average currents clearly distinguishes a non-equilibrium steady state from an equilibrium system; it is thus reasonable that a relation between currents and the entropy production should exist. By contrast, the average of state-dependent observables is independent of time both in equilibrium and non-equilibrium steady states, intuitively, it seems that such observables can provide no additional information about the steady state entropy production. As the main result of this article, we show that this intuitive notion is not correct. We can exploit the correlations between a state-dependent observable q and current r to obtain a tighter version of the TUR. We formulate the TUR in terms of the transport efficiency η_R [11]

$$\eta_R = \frac{2\langle R \rangle^2}{\text{Var}_R \Delta S_{\text{irr}}} \leq 1, \quad (1)$$

where R is the time-integrated current, $\langle R \rangle$ denotes the average and Var_R the variance, and ΔS_{irr} is the total entropy production. Our main result is the bound

$$\eta_R + \chi_{R,Q}^2 \leq 1, \quad (2)$$

where Q is the time-integral of the state-dependent observable q and $\chi_{R,Q} = \text{Cov}_{R,Q} / \sqrt{\text{Var}_R \text{Var}_Q}$, with $\text{Cov}_{R,Q}$ the covariance, is the Pearson correlation coefficient, which satisfies $-1 \leq \chi \leq 1$. As a consequence,

we obtain a tighter bound on the entropy production

$$\frac{\langle R \rangle^2}{\text{Var}_R} \leq \frac{\langle R \rangle^2}{\text{Var}_R(1 - \chi_{R,Q})} \leq \frac{1}{2} \Delta S_{\text{irr}}, \quad (3)$$

where the leftmost expression corresponds to the TUR. Surprisingly, the observable Q can be almost arbitrary, as long as it is the time-integral of a quantity which only depends on the state of the system. This implies that virtually any additional observable that can be obtained from a measurement may be used to tighten the TUR. As we show below, a tight bound is generally obtained when Q is chosen as the local average value of R .

When applying Eq. (2) to a model for the F₁-ATPase molecular motor [21], we find that, while the bound obtained on the entropy production using the TUR for the displacement of the motor is only around 40% of the actual value, measuring the time-integrated local mean velocity in addition to the displacement and using Eq. (2) yields an estimate that is about 90% accurate over a wide range of parameters. Importantly, Eq. (2) can be evaluated using only the experimentally obtained trajectory data and does not require any additional information about the parameters of the model. This suggests that taking into account correlations between observables may indeed be crucial to obtaining accurate estimates of the entropy production in terms of experimentally accessible quantities.

II. MULTIDIMENSIONAL FRI AND MONOTONICITY OF INFORMATION.

The mathematical basis of our results is an extension of the fluctuation-response inequality (FRI) [22] to multiple observables, similar to the multidimensional TUR [23]. The FRI gives an upper bound on the ratio $\mathcal{Q}(r)$ between the response of the average of an observable r to a small perturbation of the system, and its fluctuations in the unperturbed system,

$$\frac{(\delta \langle R \rangle)^2}{\text{Var}_R} \leq 2D_{\text{KL}}(\tilde{p}||p). \quad (4)$$

Here, $\delta \langle R \rangle = \widetilde{\langle R \rangle} - \langle R \rangle$ is the response of the observable R to the perturbation which changes the probability density describing the system from p to \tilde{p} and $D_{\text{KL}}(\tilde{p}||p)$ is the Kullback-Leibler divergence between the probability densities. When we consider the perturbation to be described by a parameter θ , such that $p = p^\theta$ and $\tilde{p} = p^{\theta+d\theta}$, then this is equivalent to the Cramér-Rao inequality [24, 25]

$$\frac{(\partial_\theta \langle R \rangle)^2}{\text{Var}_R} \leq I(\theta), \quad (5)$$

where $I(\theta)$ is the Fisher information

$$I(\theta) = \int d\omega (\partial_\theta \ln p^\theta(\omega))^2 p^\theta(\omega). \quad (6)$$

With this identification, we can use the Cramér-Rao inequality for vector-valued observables, $\mathbf{R}^{(K)} = (R_1, R_2, \dots, R_K)$,

$$\mathcal{Q}_R^{(K)} \equiv (\partial_\theta \langle \mathbf{R}^{(K)} \rangle)^T (\Xi_R^{(K)})^{-1} (\partial_\theta \langle \mathbf{R}^{(K)} \rangle) \leq I(\theta), \quad (7)$$

where the superscript T denotes transposition and $\Xi_R^{(K)}$ is the covariance matrix with entries $(\Xi_R^{(K)})_{ij} = \text{Cov}_{R_i, R_j}$. Note that here we assumed that the observables not linearly dependent such that the covariance matrix is positive definite. As noted in Ref. [23], Eq. (7) is the extension of the FRI to more than one observable.

Next, we want to show that increasing the number of observables results in a tighter bound, i. e. that $\mathcal{Q}_R^{(K)}(R) \leq \mathcal{Q}_R^{(K+1)}(R)$. We write the covariance matrix $\Xi_R^{(K+1)}$ of $K+1$ observables as

$$\Xi_R^{(K+1)} = \begin{pmatrix} \mathbf{A} & \mathbf{b} \\ \mathbf{b}^T & c \end{pmatrix} \quad \text{with} \quad (8)$$

$$\mathbf{A} = \Xi_R^{(K)}, \quad b_k = \text{Cov}_{R_k, R_{K+1}}, \quad c = \text{Var}_{R_{K+1}}.$$

We compute its inverse using the block-inversion formula

$$(\Xi_R^{(K+1)})^{-1} = \begin{pmatrix} \mathbf{A}^{-1} & 0 \\ 0 & 0 \end{pmatrix} + \mathbf{D} \quad (9)$$

$$\text{with } \mathbf{D} = \frac{c - \mathbf{b}^T \mathbf{A}^{-1} \mathbf{b}}{(\mathbf{A}^{-1} \mathbf{b})^T (\mathbf{A}^{-1} \mathbf{b})} \mathbf{d} \mathbf{d}^T, \quad \mathbf{d} = \begin{pmatrix} -(\mathbf{A}^{-1} \mathbf{b})^T \\ 1 \end{pmatrix}.$$

Further, we have the Schur determinant identity

$$\det(\Xi_R^{(K+1)}) = \det(\Xi_R^{(K)}) (c - \mathbf{b}^T \mathbf{A}^{-1} \mathbf{b}). \quad (10)$$

Since $\Xi_R^{(K+1)}$ and $\Xi_R^{(K)}$ are positive definite, the second factor on the right-hand side is also positive. As a consequence, the matrix \mathbf{D} in Eq. (9) is positive semi-definite and we have for any $(K+1)$ -vector $\mathbf{v}^{(K+1)}$,

$$\begin{aligned} \mathbf{v}^{(K+1),T} \Xi_R^{(K+1)} \mathbf{v}^{(K+1)} & \\ &= \mathbf{v}^{(K),T} \Xi_R^{(K)} \mathbf{v}^{(K)} + \mathbf{v}^{(K+1),T} \mathbf{D} \mathbf{v}^{(K+1)} \\ &\geq \mathbf{v}^{(K),T} \Xi_R^{(K)} \mathbf{v}^{(K)}, \end{aligned} \quad (11)$$

where $\mathbf{v}^{(K)}$ is the vector $\mathbf{v}^{(K+1)}$ with the $(K+1)$ -th component removed. For $\mathbf{v}^{(K+1)} = \partial_\theta \langle \mathbf{R}^{(K+1)} \rangle$ this yields the desired inequality

$$\mathcal{Q}_R^{(K+1)} \geq \mathcal{Q}_R^{(K)}. \quad (12)$$

In light of the Cramér-Rao inequality Eq. (7), this means that considering more observables yields more information about the parameter θ (i. e. the perturbation) and thus a tighter lower bound on the Fisher information. In that sense, the information obtained from a measurement increases monotonically with increasing the number of measured observables. This holds true only as long as the additional observables are not linearly dependent on the existing ones; if this is not the case, then the covariance matrix becomes singular and the bound saturates,

as the additional observables do not contain any new information.

In the case of two observables Q and R , the inverse of the covariance matrix can be computed explicitly and we obtain the bound

$$\frac{(\partial_\theta \langle R \rangle)^2 \text{Var}_Q - 2(\partial_\theta \langle R \rangle)(\partial_\theta \langle Q \rangle) \text{Cov}_{Q,R} + (\partial_\theta \langle Q \rangle)^2 \text{Var}_R}{\text{Var}_Q \text{Var}_R - \text{Cov}_{R,Q}^2} \leq I(\theta). \quad (13)$$

This expression simplifies further if Q is a conserved quantity with respect to the perturbation, $\partial_\theta \langle Q \rangle = 0$. Then, we find

$$\frac{(\partial_\theta \langle R \rangle)^2}{\text{Var}_R(1 - \chi_{R,Q^2})} \leq I(\theta). \quad (14)$$

In this case it is obvious that the bound is tighter than Eq. (5). This shows that, even if the average of Q contains no information about the parameter θ and the perturbation, we may still use its correlations with R to obtain a tighter version of the Cramér-Rao inequality and thus the FRI.

III. CONTINUOUS TIME-REVERSAL AND TUR.

When we consider the steady state of either an overdamped Langevin or Markov jump dynamics, it has been shown in Ref. [13] that there exists a continuous time-reversal operation parameterized by $\theta \in [-1, 1]$. This operation has the property that $\theta = 1$ corresponds to the time-forward dynamics, while $\theta = -1$ represents the time-reversed dynamics [26]. In view of later applications, we slightly generalize the discussion to a Langevin dynamics in \mathbb{R}^N with an internal degree of freedom

$$\dot{\mathbf{x}}(t) = \mathbf{a}_i(\mathbf{x}(t)) + \mathbf{G}_i \boldsymbol{\xi}(t), \quad (15)$$

where the drift vector $\mathbf{a}_i(\mathbf{x})$ and diffusion matrix \mathbf{G}_i depend on the discrete state $i = 1, \dots, M$. The dynamics of the discrete state are governed by a Markov jump process with transition rates $W_{ij}(\mathbf{x})$ from state j to state i . We take the diffusion matrix to be independent of the position in order to simplify some of the following notation, however, the extension to a position-dependent diffusion matrix can be readily obtained. The evolution of the probability density $p_i(\mathbf{x}, t)$ for being at position \mathbf{x} and in state i at time t is governed by the Fokker-Planck master equation

$$\begin{aligned} \partial_t p_i(\mathbf{x}, t) = & -\nabla \cdot (\mathbf{a}_i(\mathbf{x}) - \nabla^T \mathbf{B}_i) p_i(\mathbf{x}, t) \\ & + \sum_j (W_{ij}(\mathbf{x}) p_j(\mathbf{x}, t) - W_{ji}(\mathbf{x}) p_i(\mathbf{x}, t)), \end{aligned} \quad (16)$$

where $\mathbf{B}_i = 2\mathbf{G}_i \mathbf{G}_i^T$ is assumed to be positive definite (i. e. \mathbf{G}_i should have full rank). This dynamics reduces

to a pure Langevin dynamics in absence of the discrete degree of freedom and to a pure Markov jump dynamics if there is no dependence on \mathbf{x} . For this type of dynamics, we may consider two flavors of currents [27]

$$R_d = \int_0^\tau dt \boldsymbol{\rho}_i^T(\mathbf{x}(t)) \circ \dot{\mathbf{x}}(t), \quad (17a)$$

$$R_j = \int_0^\tau \phi_{i(t+dt),j(t)}(\mathbf{x}(t)). \quad (17b)$$

Here $\boldsymbol{\rho}_i(\mathbf{x})$ is a differentiable vector field, $\phi_{ij}(\mathbf{x}) = -\phi_{ji}(\mathbf{x})$ are the entries of an antisymmetric matrix and \circ denotes the Stratonovich product. Intuitively, the diffusive current R_d may be interpreted as a generalized displacement, in which the velocity is weighted by the position- and state-dependent function $\boldsymbol{\rho}_i(\mathbf{x})$. The jump current R_j , on the other hand, counts transitions between different states, which are weighted by the function $\phi_{ij}(\mathbf{x})$. The averages of these quantities in the steady state are proportional to time and given by

$$\langle R_d \rangle = \tau \sum_i \int d\mathbf{x} \boldsymbol{\rho}_i^T(\mathbf{x}(t)) (\mathbf{a}_i(\mathbf{x}) - \nabla^T \mathbf{B}_i) p_{i,\text{st}}(\mathbf{x}), \quad (18a)$$

$$\langle R_j \rangle = \tau \sum_{ij} \int d\mathbf{x} \phi_{ij}(\mathbf{x}) W_{ij}(\mathbf{x}) p_{j,\text{st}}(\mathbf{x}). \quad (18b)$$

A crucial property of these currents is that their averages are rescaled by the continuous time-reversal operation:

$$\langle R \rangle^\theta = \theta \langle R \rangle. \quad (19)$$

This implies that $\partial_\theta \langle R \rangle^\theta = \langle R \rangle$. Further, the Fisher information corresponding to the path probabilities of the dynamics parameterized by θ is related to the entropy production [13, 22, 28],

$$I(\theta) \leq \frac{1}{2} \Delta S_{\text{irr}}, \quad (20)$$

where equality holds for a pure Langevin dynamics. With this, Eq. (7) implies the multidimensional TUR [23],

$$\langle \mathbf{R}^{(K)} \rangle^T (\boldsymbol{\Xi}_R^{(K)})^{-1} \langle \mathbf{R}^{(K)} \rangle \leq \frac{1}{2} \Delta S_{\text{irr}}, \quad (21)$$

where the components of $\mathbf{R}^{(K)}$ are currents of either type in Eq. (17). The new insight from the preceding discussion is that the left-hand side increases monotonically

when increasing the number of measured currents. This fact is very useful when we want to use the left-hand side to estimate the entropy production: Any additional information that can be obtained from a measurement can be used to improve the estimate.

Crucially, this is not restricted to current observables. To see this, we note that the steady state probability density $p_{i,\text{st}}(\mathbf{x})$ is invariant under changing the parameter θ [13]. As a consequence, for a state-dependent (or non-current) observable Q

$$Q = \int_0^\tau dt q_{i(t)}(\mathbf{x}(t), t), \quad (22)$$

where the function $q_i(\mathbf{x}, t)$ may depend on the position, the internal state and time, its average does not depend on θ

$$\langle Q \rangle^\theta = \langle Q \rangle. \quad (23)$$

Thus, $\partial_\theta \langle Q \rangle^\theta = 0$, and we may include such observables in Eq. (21) by setting the corresponding entries in the vector $\langle \mathbf{R}^{(K)} \rangle$ to zero. However, such observables do contribute to the covariance matrix $\Xi_R^{(K)}$, and Eq. (12) guarantees that the resulting bound will be tighter than the one without these observables. For the case of one current and one state-dependent observable, we may use Eq. (14) to write the bound explicitly

$$\frac{\langle R \rangle^2}{\text{Var}_R(1 - \chi_{R,Q})} \leq \frac{1}{2} \Delta S_{\text{irr}}, \quad (24)$$

which is equivalent to Eq. (2). This is very appealing from an experimental point of view: Currents as in Eq. (17) depend on the velocity or transitions between the internal states. Since observing these requires a high time-resolution, such quantities are generally challenging to measure accurately. The only exception are specific choices of the weighting functions, for which the time-integrated observable can be measured directly, for example the displacement of a particle. By contrast, observables of the type Eq. (22), which depend only on the position and the internal state can easily be evaluated from trajectory data. Eq. (24) implies that, provided at least one current can be obtained from the measurement, we may use other, non-current observables to improve the lower bound on the entropy production.

IV. OPTIMAL OBSERVABLES AND STOCHASTIC ENTROPY PRODUCTION.

Given that the choice of the observable Q in Eq. (24) has a lot of freedom, a natural question is whether there exists an optimal observable which maximizes the bound. This is equivalent to finding Q such that magnitude of the Pearson coefficient $\chi(R, Q)$ becomes maximal for given R . Unfortunately, we have not been able to solve this optimization problem in general. However, there is one particular case, where we can obtain the solution explicitly.

For a pure Langevin dynamics without internal states, we may consider the stochastic entropy production Σ as the observable R . This corresponds to the weighting function

$$\begin{aligned} \rho(\mathbf{x}) &= \mathbf{B}^{-1} \boldsymbol{\nu}_{\text{st}}(\mathbf{x}) \quad \text{with} \\ \boldsymbol{\nu}_{\text{st}}(\mathbf{x}) &= \mathbf{a}(\mathbf{x}) - \nabla^T \mathbf{B} \ln p_{\text{st}}(\mathbf{x}). \end{aligned} \quad (25)$$

The quantity $\boldsymbol{\nu}_{\text{st}}(\mathbf{x})$ is called local mean velocity. As we show in the SM, in this case, the optimal choice for Q is

$$Q = \bar{\Sigma} = \int_0^\tau dt \boldsymbol{\nu}_{\text{st}}^T(\mathbf{x}(t)) \mathbf{B}^{-1} \boldsymbol{\nu}_{\text{st}}(\mathbf{x}(t)). \quad (26)$$

This quantity can be interpreted as a local mean entropy production, i. e. the expected entropy production rate at position $\mathbf{x}(t)$ integrated along the trajectory. Note that both Σ and $\bar{\Sigma}$ have the entropy production ΔS_{irr} as their average value. As it turns out, this choice turns Eq. (24) into an equality,

$$2\Delta S_{\text{irr}} = \text{Var}_\Sigma(1 - \chi_{\Sigma, \bar{\Sigma}}^2), \quad (27)$$

which shows that this really is the optimal choice of Q . We remark that this equality is equivalent to the equality $2\Delta S_{\text{irr}} = \text{Var}(\delta\Sigma)$ with $\delta\Sigma = \Sigma - \bar{\Sigma}$ derived in Ref. [13]. For general currents, while the optimal Q could not be obtained explicitly, we note that the average current is expressed in terms of the local mean velocity as

$$\langle R \rangle = \tau \int d\mathbf{x} \boldsymbol{\rho}^T(\mathbf{x}) \boldsymbol{\nu}_{\text{st}}(\mathbf{x}) p_{\text{st}}(\mathbf{x}). \quad (28)$$

Comparing this to Eq. (26), this suggests that a good choice for Q may be

$$Q = \bar{R} = \int_0^\tau dt \boldsymbol{\rho}^T(\mathbf{x}(t)) \boldsymbol{\nu}_{\text{st}}(\mathbf{x}(t)). \quad (29)$$

This choice is the local mean value of the current, which has the same average as the current itself.

Further insight into the meaning of the optimal observable Q can be gained from the following consideration. Since the average of the observables R and $\bar{R} = R - Q$ exhibit the same scaling under continuous time-reversal

$$\partial_\theta \langle R \rangle^\theta = \partial_\theta \langle \bar{R} \rangle^\theta = \langle R \rangle, \quad (30)$$

they both satisfy a TUR

$$\frac{\langle R \rangle^2}{\text{Var}_R} \leq \frac{1}{2} \Delta S_{\text{irr}} \quad \text{and} \quad \frac{\langle R \rangle^2}{\text{Var}_{\bar{R}}} \leq \frac{1}{2} \Delta S_{\text{irr}}. \quad (31)$$

Since the choice of Q is arbitrary within the class of observables Eq. (22), we may minimize the variance of \bar{R} with respect to Q ,

$$\frac{\langle R \rangle^2}{\inf_Q (\text{Var}_{\bar{R}})} \leq \frac{1}{2} \Delta S_{\text{irr}}. \quad (32)$$

We may generalize this slightly by choosing $\tilde{R} = R - \alpha Q$, where α is a constant. In this case, the minimization with respect to α can be done explicitly and yields

$$\inf_\alpha (\text{Var}_{\tilde{R}}) = \text{Var}_R(1 - \chi_{R,Q}^2), \quad (33)$$

from which we readily obtain Eq. (24) and finding the optimal observable corresponds to maximizing the Pearson coefficient. Intuitively, the optimal observable is the state-dependent observable whose fluctuations most closely mimic those of the current R , thus minimizing the variance of $R - Q$. As a consequence, we may interpret Eq. (2) as follows: The maximal transport efficiency η_R for a given current is limited by how closely the statistics of the current can be emulated using a non-current observable. If we can find a non-current observable Q that behaves very similar to the current, the corresponding Pearson coefficient is large and we cannot reach a large transport efficiency. On the other hand, if no such observable exists, then the maximal Pearson coefficient is small and we can in principle realize a transport efficiency close to unity.

An extreme case is the observable $\delta\Sigma$, i. e. the stochastic entropy production relative to its local mean value introduced above. Since this choice turns the TUR into an equality, this implies

$$\text{Cov}_{\delta\Sigma, Q} = 0 \quad (34)$$

for any state-dependent observable Q . On the other hand, we have by considering Eq. (21) for $\delta\Sigma$ and a current R (see also Eq. (14))

$$(\text{Cov}_{\delta\Sigma, R} - 2\langle R \rangle)^2 \leq 0, \quad (35)$$

where we used $\text{Var}_{\delta\Sigma} = 2\Delta S_{\text{irr}}$. This implies

$$\text{Cov}_{\delta\Sigma, R} = 2\langle R \rangle \quad (36)$$

for any current R . Thus, the stochastic entropy production relative to the local mean value serves as a projector on the current part of an observable in the sense that, if we have $\tilde{R} = R - Q$ with R as in Eq. (17) and Q as in Eq. (22), then

$$\frac{1}{2}\text{Cov}_{\delta\Sigma, \tilde{R}} = \langle R \rangle. \quad (37)$$

This relation is actually sufficient to derive the TUR Eq. (31) since

$$\begin{aligned} 1 \leq \chi_{\delta\Sigma, \tilde{R}}^2 &= \frac{\text{Cov}_{\delta\Sigma, \tilde{R}}^2}{\text{Var}_{\delta\Sigma} \text{Var}_{\tilde{R}}} = \frac{\text{Cov}_{\delta\Sigma, \tilde{R}}^2}{\text{Cov}_{\delta\Sigma, \delta\Sigma} \text{Var}_{\tilde{R}}} \\ &= \frac{\text{Cov}_{\delta\Sigma, \tilde{R}}^2}{\text{Cov}_{\delta\Sigma, \Sigma - \bar{\Sigma}} \text{Var}_{\tilde{R}}} = \frac{(2\langle R \rangle)^2}{2\langle \Sigma \rangle \text{Var}_{\tilde{R}}} \\ &= \frac{2\langle R \rangle^2}{\Delta S_{\text{irr}} \text{Var}_{\tilde{R}}}. \end{aligned} \quad (38)$$

V. DEMONSTRATION: MOLECULAR MOTOR MODEL

To demonstrate how Eq. (24) may be used to obtain a tight bound on the entropy production, we consider the

model for the F₁-ATPase molecular motor introduced in Ref. [21]. This model describes the motion of a probe bead coupled to a rotating molecular motor. The probe is considered to be trapped inside a potential $U_i(x)$, which is due to the joint between the probe and the motor and the internal structure of the motor. As the motor rotates in steps of length L , the potential depends on the current state of the motor as $U_i(x) = U_0(x - iL)$. In the simplest form of the model, the trapping potential is harmonic, $U_0(x) = kx^2/2$, and the motor rotates in steps of $L = 120^\circ$. The transitions between the states of the motor are described by the position-dependent transition rates

$$\begin{aligned} W_i^+ &= W_0 \exp\left[\frac{\alpha}{k_B T} (U_i(x) - U_{i+1}(x) + \Delta\mu)\right], \\ W_{i+1}^- &= W_0 \exp\left[\frac{1-\alpha}{k_B T} (U_i(x) - U_{i+1}(x) + \Delta\mu)\right], \end{aligned} \quad (39)$$

where W_i^+ (W_{i+1}^-) is the rate of transitions from i to $i+1$ (from $i+1$ to i). Here, W_0 quantifies the overall activity of the motor, $\Delta\mu$ is the chemical potential difference driving the rotation and $0 \leq \alpha \leq 1$ is a parameter characterizing the asymmetry of the position-dependence of the rates. Aside from the transition rates, the other parameters entering Eq. (15) are $a_i(x) = (-U_i'(x) - F)/\gamma$, where γ is the friction coefficient, F is an external force acting on the probe, and $G = \sqrt{2k_B T/\Gamma}$. An experimentally accessible current is the total displacement of the probe,

$$z = \int_0^\tau dt \dot{x}(t). \quad (40)$$

Because the system is effectively one-dimensional, the local mean velocity in the steady state is given by $\nu_{\text{st}}(x) = 1/(\tau_0 p_{\text{st}}(x))$, where τ_0 is a constant with dimensions of time and $p_{\text{st}}(x)$ is the L -periodic steady state probability density. In this case, we can thus reconstruct the local mean velocity from the trajectory data of the probe by taking a histogram of the probe positions. We then define the observable

$$Q = \int_0^\tau dt \frac{1}{p_{\text{st}}(x(t))}, \quad (41)$$

which is proportional to \bar{z} . Since the proportionality factor $1/\tau_0$ cancels in the Pearson coefficient, Q and \bar{z} are equivalent with respect to Eq. (24). To assess the tightness of the various inequalities, we introduce the transport efficiencies

$$\begin{aligned} \eta_z &= \frac{2\langle z \rangle^2}{\text{Var}_z \Delta S_{\text{irr}}}, \\ \eta_{z, \bar{z}} &= \frac{2\langle z \rangle^2}{\text{Var}_z \Delta S_{\text{irr}} (1 - \chi_{z, \bar{z}}^2)}. \end{aligned} \quad (42)$$

Both of these quantities are smaller than unity and measure the magnitude of the average transport relative to its fluctuations and the dissipation. The efficiencies Eq. (42) are shown for the molecular motor model in Fig. 1 as a

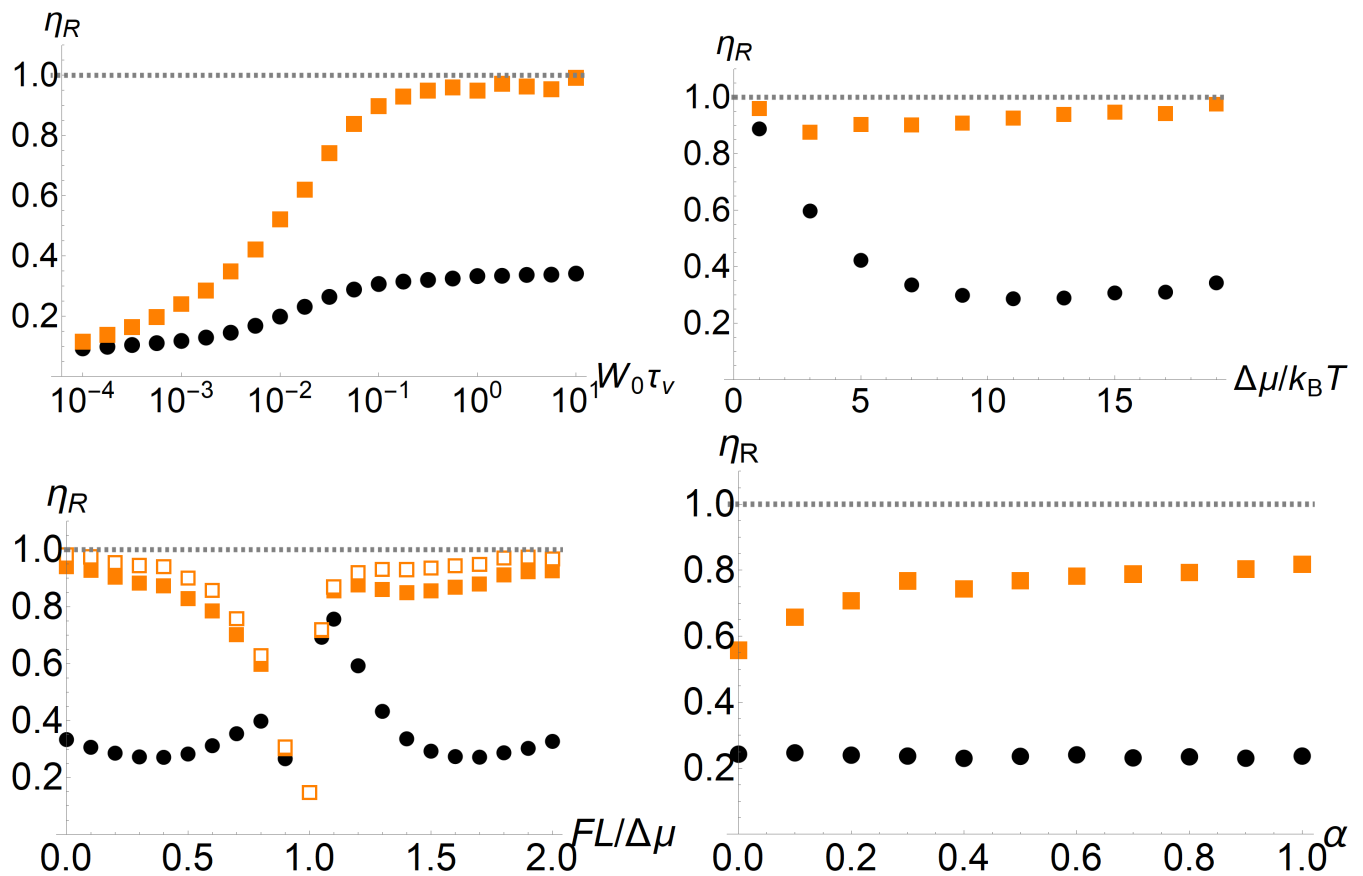


FIG. 1. The transport efficiency Eq. (42) for the displacement of the probe attached to the molecular motor as a function of different parameters. The black circles correspond to the TUR for the displacement z only, while the solid orange squares show Eq. (24) including the correlations between the displacement and its local mean value \bar{z} . The data are obtained by numerical simulations of Eq. (15) with $W_0\tau_v = 10$, $U_0 = 50k_B T$, $\Delta\mu = 19k_B T$, $\alpha = 0.1$ and $\gamma = 2.5 \cdot 10^3$, except where noted differently. (Top left) As a function of the base activity W_0 . The horizontal axis is scaled by the timescale $\tau_v = \gamma k_B T / (kL)^2$ [21]. (Top right) As a function of the chemical potential difference $\Delta\mu$. (Bottom left) As a function of the external load F . The empty orange squares are Eq. (24) with a numerically optimized observable, see Eq. (43). (Bottom right) As a function of the asymmetry parameter α .

function of various parameters. The top-left panel shows η_R as a function of the base activity W_0 , which corresponds to the concentration of ATP in the experiment. For small activity both η_z and $\eta_{z,\bar{z}}$ are comparable and small; in this limit, the transitions between the different motor conformations are not translated efficiently into motion and the dissipation is not reflected in the motion of the probe [21]. For large activity, η_z saturates at a value of around 0.4. However, when we compute $\eta_{z,\bar{z}}$ in this regime, we find that it saturates at a value close to unity, i. e. the maximum possible value. The top-right panel shows η as a function of the chemical potential difference $\Delta\mu$. While this value cannot be readily changed in experiment, it yields important insight into the nature of the bound Eq. (24). For small $\Delta\mu$ the system is almost in equilibrium, and both the TUR and Eq. (24) are close to an equality. However, as we drive the system out of equilibrium, the TUR ratio quickly drops, while Eq. (24) remains close to unity. This suggests that, while the TUR

is generically only saturated close to equilibrium [4, 29], the improved bound Eq. (24) can yield an accurate estimate of the entropy production even far from equilibrium. The bottom-left panel shows η as a function of the external load force. Close to the stall condition $FL = \Delta\mu$ neither of the bounds is tight. This is reasonable, since when the motor stalls, also the probe stops moving, while the motor keeps changing its conformation and thus dissipating energy. Interestingly, both bounds are close to unity slightly above the stall condition, i. e. when the external load is just strong enough to turn the motor in the opposite direction. Away from the stall condition, we again find that the TUR is rather loose, while the improved bound Eq. (24) remains tight. Note that in this panel we also included the results obtained by optimizing

the observable Q . Specifically, we write

$$\tilde{z} = \int_0^\tau dt \sum_{k=1}^K \left(a_k \sin\left(\frac{2\pi x(t)}{L}\right) + b_k \cos\left(\frac{2\pi x(t)}{L}\right) \right) \quad (43)$$

and then numerically optimize the parameters a_k , b_k such that $\chi(z, \tilde{z})^2$ is maximal for the given trajectory data. Here we use $K = 10$; further increasing of the number of parameters provides no notable improvement. The numerical optimization is done using Mathematica's `NMaximize` command. The result are the empty orange squares in the bottom-left panel of Fig. 1. As can be seen, the observable \tilde{z} is not truly optimal, so that some improvement of the lower bound on entropy production is possible. However, the heuristic choice \bar{z} already provides a useful estimate without the need for any parameter optimization. Finally, the bottom-right panel shows η as a function of the asymmetry parameter α . As was shown in Ref. [21] the motor can operate without internal dissipation close to $\alpha = 0$, whereas other values of α result in a finite amount of internal dissipation. Since this difference is most pronounced at low activity, we choose W_0 such that the velocity remains constant at $v = 0.65v_{\max}$ for all values of α ; this corresponds to $W_0\tau_v \approx 10^{-2}$ in the top-left panel. While in this regime of low activity, neither bound is saturated, Eq. (24) does yield a considerable improvement over the TUR. Interestingly, neither bound shows a pronounced dependence on α , which indicates that their tightness is not related to the amount of internal vs. external dissipation. In summary, we find that the TUR is generally not tight for this model, which mirrors the behavior in other types of molecular motors [14]. Viewed on its own, this would suggest that F₁-ATPase is not efficient at saturating the bound set by the TUR. However, when we take into account the correlations between the velocity and its local mean value in Eq. (24), the resulting inequality is almost saturated. Thus, in reality, the motor operates close to the limit permitted by the thermodynamic bound in the biologically relevant parameter regime.

VI. DISCUSSION

In this article, we have shown how to improve the TUR by taking into account the correlations between current and non-current observables and that the resulting inequality can yield a much improved estimate of entropy production. We remark that Eq. (14) is actually more general: It allows us to improve any bound provided by the FRI, provided that we can find a quantity whose average is invariant under the perturbation. Since many generalizations of the TUR may be derived from the FRI [17–20, 30], these generalizations can be improved in a completely analogous manner, by exploiting the existence of symmetries and conserved quantities. This is a mani-

festation of the monotonicity of information established in Eq. (12).

Similar to the example of a molecular motor discussed above, we can give a heuristic recipe for improving the TUR, which is expected to work well whenever the system is dominated by a single, essentially one-dimensional current. The idea is that in this case, we expect the local mean current to be approximately inversely proportional to the inverse occupation fraction. This allows us to obtain a reasonable choice for the observable Q by i) determining the empirical occupation fraction of a suitably discretized state space from the trajectory data (i. e. how many data points N_k of the trajectory data are in state k), ii) evaluating $Q = \sum_i 1/N_{k(t_i)}$ along each trajectory, where $k(t_i)$ is the state at time t_i and iii) computing the Pearson coefficient between Q and the time-integrated current R . We stress that this recipe relies only on the existing trajectory data and does not require any assumptions about the dynamics or parameters.

For dynamics with several or higher-dimensional currents, the time-integrated inverse occupation fraction is not necessarily a good choice for the observable Q , since the inverse proportionality between the occupation fraction and the local mean velocity is no longer valid. However, since any choice of Q yields a valid bound, we may still employ Eq. (29), even if the local mean velocity is not known precisely. One approach might be to use an approximation (or even just educated guess) for the local mean velocity. We anticipate that this may be useful for example for systems with disorder. Provided that the disorder is not too strong, we may use the disorder-free local mean velocity in Eq. (29) and still expect to obtain a reasonable improvement over the TUR. In the presence of several currents, it is only possible to estimate the partial entropy production corresponding to the measured current [6, 31]; in such situations, measuring several currents and state-dependent observables is required to obtain a good estimate on the entropy production using Eq. (21).

Finally, the fact that the model of F₁-ATPase is close to saturating the bound Eq. (24) allows for a bit of intriguing speculation: If a similar finding can be confirmed for other models of molecular motors, this may imply that saturating thermodynamic inequalities can be a source of evolutionary pressure. This appears reasonable in the light of interpreting Eq. (24) as a transport efficiency, Eq. (42): Achieving precise transport at minimal dissipation would obviously be advantageous for any machine, whether artificial or naturally occurring. However, we leave further investigation of this question to future work.

ACKNOWLEDGMENTS

Acknowledgments. This work was supported by KAKENHI (Nos. 17H01148, 19H05795 and 20K20425).

-
- [1] K. Sekimoto, *Stochastic Energetics*, Lecture Notes in Physics (Springer Berlin Heidelberg, 2010).
- [2] U. Seifert, Stochastic thermodynamics, fluctuation theorems and molecular machines, Rep. Prog. Phys. **75**, 126001 (2012).
- [3] T. Harada and S.-i. Sasa, Equality connecting energy dissipation with a violation of the fluctuation-response relation, Phys. Rev. Lett. **95**, 130602 (2005).
- [4] J. Li, J. M. Horowitz, T. R. Gingrich, and N. Fakhri, Quantifying dissipation using fluctuating currents, Nature Comm. **10**, 1 (2019).
- [5] S. K. Manikandan, D. Gupta, and S. Krishnamurthy, Inferring entropy production from short experiments, Phys. Rev. Lett. **124**, 120603 (2020).
- [6] S. Otsubo, S. Ito, A. Dechant, and T. Sagawa, Estimating entropy production by machine learning of short-time fluctuating currents, Phys. Rev. E **101**, 062106 (2020).
- [7] T. Van Vu, V. T. Vo, and Y. Hasegawa, Entropy production estimation with optimal current, Phys. Rev. E **101**, 042138 (2020).
- [8] J. M. Horowitz and T. R. Gingrich, Thermodynamic uncertainty relations constrain non-equilibrium fluctuations, Nature Phys. **16**, 15 (2020).
- [9] A. C. Barato and U. Seifert, Thermodynamic uncertainty relation for biomolecular processes, Phys. Rev. Lett. **114**, 158101 (2015).
- [10] T. R. Gingrich, J. M. Horowitz, N. Perunov, and J. L. England, Dissipation bounds all steady-state current fluctuations, Phys. Rev. Lett. **116**, 120601 (2016).
- [11] A. Dechant and S.-i. Sasa, Current fluctuations and transport efficiency for general Langevin systems, J. Stat. Mech. Theory E. **2018**, 063209 (2018).
- [12] P. Pietzonka, F. Ritort, and U. Seifert, Finite-time generalization of the thermodynamic uncertainty relation, Phys. Rev. E **96**, 012101 (2017).
- [13] A. Dechant and S. i. Sasa, Continuous time-reversal and equality in the thermodynamic uncertainty relation (2020), arXiv:2010.14769 [cond-mat.stat-mech].
- [14] W. Hwang and C. Hyeon, Energetic costs, precision, and transport efficiency of molecular motors, J. Phys. Chem. Lett. **9**, 513 (2018).
- [15] A. Dechant and S.-i. Sasa, Entropic bounds on currents in Langevin systems, Phys. Rev. E **97**, 062101 (2018).
- [16] S. Pal, S. Saryal, D. Segal, T. S. Mahesh, and B. K. Agarwalla, Experimental study of the thermodynamic uncertainty relation, Phys. Rev. Research **2**, 022044(R) (2020).
- [17] K. Liu, Z. Gong, and M. Ueda, Thermodynamic uncertainty relation for arbitrary initial states, Phys. Rev. Lett. **125**, 140602 (2020).
- [18] T. Koyuk and U. Seifert, Operationally accessible bounds on fluctuations and entropy production in periodically driven systems, Phys. Rev. Lett. **122**, 230601 (2019).
- [19] T. Koyuk and U. Seifert, Thermodynamic uncertainty relation for time-dependent driving, Phys. Rev. Lett. **125**, 260604 (2020).
- [20] T. Van Vu and Y. Hasegawa, Thermodynamic uncertainty relations under arbitrary control protocols, Phys. Rev. Research **2**, 013060 (2020).
- [21] K. Kawaguchi, S. i. Sasa, and T. Sagawa, Nonequilibrium dissipation-free transport in f1-atpase and the thermodynamic role of asymmetric allostereism, Biophys. J. **106**, 2450 (2014).
- [22] A. Dechant and S.-i. Sasa, Fluctuation–response inequality out of equilibrium, Proc. Natl. Acad. Sci. **117**, 6430 (2020).
- [23] A. Dechant, Multidimensional thermodynamic uncertainty relations, J. Phys. A Math. Theor. **52**, 035001 (2018).
- [24] C. Radhakrishna Rao, Information and the accuracy attainable in the estimation of statistical parameters, Bull. Calcutta Math. Soc. **37**, 81 (1945).
- [25] H. Cramér, *Mathematical methods of statistics*, Vol. 9 (Princeton university press, 2016).
- [26] S.-i. Sasa, Possible extended forms of thermodynamic entropy, J. Stat. Mech. Theory E. **2014**, P01004 (2014).
- [27] R. Chetrite and H. Touchette, Nonequilibrium Markov processes conditioned on large deviations, Ann. Henri Poincaré **16**, 2005 (2015).
- [28] Y. Hasegawa and T. Van Vu, Uncertainty relations in stochastic processes: An information inequality approach, Phys. Rev. E **99**, 062126 (2019).
- [29] K. Macieszczak, K. Brandner, and J. P. Garrahan, Unified thermodynamic uncertainty relations in linear response, Phys. Rev. Lett. **121**, 130601 (2018).
- [30] I. Di Terlizzi and M. Baiesi, Kinetic uncertainty relation, J. Phys. A Math. Theor. **52**, 02LT03 (2018).
- [31] M. Polettoni, A. Lazarescu, and M. Esposito, Tightening the uncertainty principle for stochastic currents, Phys. Rev. E **94**, 052104 (2016).